CHAPTER 11

Evaluation of Macular Perfusion in Successfully Reattached Macula-off Diabetic Tractional Retinal Detachment

Miguel A. Quiroz-Reyes, MD[1,*], Erick A. Quiroz-Gonzalez[1,2], Jorge Morales-Navarro[2], Miguel A. Quiroz-Gonzalez[1], Margarita Montano[1], Felipe Esparza-Correa[2], Jennifer H. Kim-Lee[2], Boris Moreno-Andrade[2], Alejandra Nieto-Jordan[2], Ahmad R. Alsaber[3] and **Virgilio Lima-Gomez[4]**

[1] Oftalmologia Integral ABC, Retina Department, Medical and Surgical Assistance Institution (Nonprofit Organization), Affiliated with the Postgraduate Studies Division, National Autonomous University of Mexico, Mexico City, Mexico

[2] Institute of Ophthalmology, Fundacion Conde de Valenciana, Private Assistance Institution (Nonprofit Organization), Mexico City, Mexico

[3] Department of Mathematics and Statistics, University of Strathclyde, Glasgow, UK

[4] Ophthalmology Service, Hospital Juarez de Mexico, Public Assistance Institution (Nonprofit Organization), Mexico City, Mexico

Abstract: Current imaging techniques based on optical coherence tomography (OCT) angiography are useful for observing different retinal microcirculation patterns. The primary purpose of this chapter was to describe the functional, structural, and serial perfusion postoperative outcomes of successfully reattached macula-off tractional retinal detachment (TRD). Patients who underwent a successful diabetic vitrectomy were analyzed. The mean differences between the preoperative best-corrected visual acuity (BCVA), 3-month BCVA, and final postoperative BCVA were statistically significant ($p < 0.05$). The duration of vision loss before surgery was 11.6 ± 2.3 weeks (mean ± standard deviation (SD)).

The mean duration (± SD) of the resolution of macular detachment was 3.6 ± 1.7 weeks in the pure macular TRD group and 1.8 ± 0.8 weeks in the combined tractional and rhegmatogenous macular detachment ($p < 0.05$) group. The mean follow-up duration of all patients was 11.4 ± 5.7 months (mean ± SD). Longitudinal multimodal imaging tests revealed abnormal superficial and deep microcirculation patterns with multiple microabnormalities in the foveal avascular zone and different but distinct areas of the non-perfused macula in different OCT angiography slabs. Additionally, disorganization

[*] **Corresponding author Miguel A. Quiroz-Reyes, MD:** Oftalmologia Integral ABC, Retina Department, Medical and Surgical Assistance Institution (Nonprofit Organization), Affiliated with the Postgraduate Studies Division, National Autonomous University of Mexico, Mexico City, Mexico; Tel: +52 55 5217 2732; Fax: +52 55 1664 7180;
E-mails: drquiroz@prodigy.net.mx and drquirozreyes7@gmail.com

of the retinal inner layers and chronic ischemic macular edema were observed in 82% of eyes examined using the spectral domain (SD) OCT. Therefore, these data suggest that despite the successful anatomical reattachment of the macula, long-term postoperative microcirculatory abnormalities were detected in both groups; however, these abnormalities were predominantly accompanied by severe persistent ischemia in the recurrent TRD group due to the presence of multiple microcirculatory defects.

Keywords: Choriocapillaris subfoveal plexus, Deep vascular plexus, Disorganization of the retinal inner layers, Long-term proliferative diabetic retinopathy complications, Macula-off tractional retinal detachment, Optical coherence tomography angiography, Macular perfusion indices, Perfusion microcirculatory abnormalities, Ischemic macula, Chromatic visual field testing, Microperimetry, Multifocal electroretinography, Secondary complicated retinal detachment, Superficial vascular plexus, Vessel density.

INTRODUCTION

Diabetes mellitus (DM) is prevalent worldwide, affecting an estimated 285 million adults (6.4%) as of 2010 [1]. It is one of the main causes of visual morbidity worldwide. The estimated prevalence of diabetic retinopathy (DR) and vision-threatening DR from 2005-2008 was 28.5% and 4.4%, respectively, among US adults with diabetes [2]. The main causes of vision loss in these patients include diabetic macular edema (DME), chronic cystic macular edema (CME), and complications related to proliferative diabetic retinopathy (PDR), including recurrent vitreous hemorrhage (VH), tractional retinal detachment (TRD), refractory macular edema associated with posterior hyaloid traction, combined traction and rhegmatogenous retinal detachment, and epiretinal membrane (ERMs) proliferation. These are the most common indications for surgical vitrectomy [3 - 5].

One of the most successful techniques used to manage DR is the administration of vascular endothelial growth factor (anti-VEGF) [6]. Although they are limited by their short-lived effects, they are widely available for use worldwide, especially in the treatment of aggressive proliferative DR [6]. However, some patients are treated with steroids, periocular injections, or intravitreal extended-release devices to maintain long-term visual outcomes. Panretinal photocoagulation (PRP) remains the gold standard of care but is preferred as a second-line treatment, especially in developed countries, owing to the popularity of anti-VEGF treatments [7].

The protocol proposed by Sivaprasad *et al.* (2015) [8] for diabetic retinopathy 'Clinical efficacy and mechanistic evaluation of aflibercept for proliferative diabetic retinopathy (acronym CLARITY) and Research Network Protocol' has

been used as a guideline for the surveillance and management of patients with macular edema and complications related to Proliferative DR (PDR). When DR is detected late, advanced pars plana vitrectomy (PPV) is needed [7]. Despite extensive research, the predictive factors for visual outcomes after vitrectomy still largely remain to be elucidated [9 - 11]. Several researchers have used horizontal B-scans of optical coherence tomography (OCT) images to investigate the disorganization of the retinal inner layers (DRIL) [12]. This method was used to assess the boundaries of the ganglion cell layer-inner plexiform layer (GCL-IPL) complex, inner nuclear layer (INL), and outer plexiform layer (OPL). Sun *et al.* (2014) investigated whether DRIL predicts visual acuity (VA) in eyes with central edema (DME). They found that a greater DRIL extent at baseline correlated with worse baseline VA, and an increase in DRIL during 4 months was associated with worsening VA at 8 months [12].

OCT angiography (OCT-A) facilitates visualization of blood flow in biological tissues. It noninvasively creates *in vivo* 3-dimensional composites of separate layers of the retinal and choroidal vasculature without the use of a contrast agent [13]. Using multiple algorithms, the sensitivity of imaging methods is increased for detailed imaging of the superficial and deep retinal capillary plexus and choriocapillaris [13]. The OCT-A method ignores the quantitative measurement of blood flow and uses motion as a contrast mechanism to visualize the location of the moving cells [13]. It eliminates the need for a dye [14, 15] and the 'transit window' effect observed with fundus fluorescein angiography (FFA) and indocyanine (ICG). OCT-A also avoids dark artifacts of retinal and vascular features that may occur owing to dye leakage [16]. This technique provides capillary-level detail at high depth resolution, which is provided only by histological methods [17 - 20].

OCT-A is useful for assessing DR, as it shows retinal foveal avascular zone (FAZ) enlargement and microaneurysms, and facilitates the examination of superficial and deep capillary plexuses in several diabetic lesions. When used along with OCT-A, Optovue AngioVue system technology enables quantitative analysis of the superficial and deep plexuses of the retinal vessels, serving as biomarkers for the diagnosis and monitoring of disease progression or treatment responses [21]. Fluorescein angiography cannot resolve the details of the deep capillary plexus and peripapillary radial capillaries [16, 17, 22]. However, OCT-A is a superior method for the quantitative analysis of retinal perfusion, as it is able to detect all clinically relevant retinal findings in individuals with DR [22, 23]. Additionally, disc neovascularization (NVD) and neovascularization elsewhere (NVE) were reliably detected using OCT-A [24 - 26] (Fig. **1**). Since the assessment of these clinical findings is important for better management of DR, such as during the monitoring of medical and surgical outcomes, OCT-A

Engineering, Heidelberg, Germany and the swept-source DRI OCT Triton device by Topcon Medical Systems, Inc.). We routinely performed postoperative perfusion and quantitative vessel density (VD) and choroidal flow evaluations using an OCT-A device (RTVue XR OCT Avanti with AngioVue Software; OptoVue Inc., Fremont, CA, USA). In summary, it uses a specialized split-spectrum amplitude decorrelation angiography software algorithm and acquires 70,000 A-scans/s to compose OCT-A volumes consisting of 304 Å – 304 A-scans, achieving a high axial resolution at depths of up to 5 μm and minimizing motion artifacts. Each OCT-A cube scan comprised 304 Å – 304 A-scans within a 3 mm × 3 mm square centered on the fovea, which yielded 304 B-scans. Each B-scan output displays an average of at least two scans. Default retinal imaging settings and built-in projection artifact removal tools were used to perform image adjustment and segmentation. Segmentation of the superficial vascular plexus (SVP), deep vascular plexus (DVP), outer retinal layer, and choriocapillaris subfoveal plexus (CSP) slabs was performed using AngioVue software. Scan quality was evaluated using the standard signal strength index (SSI) provided by the software, and only scans with an SSI > 46 were considered. In a properly equipped retinal unit, postoperative multimodal functional evaluations should include final BCVA, macular retinal sensitivity (MRS), foveal retinal sensitivity (FRS), and retinal sensitivity analysis mapping (RSAM). These parameters should be assessed by microperimetry using a standard Macular Integrity Assessment System (MAIA). Microperimetry should be performed to assess the retinal sensitivity. This assessment enabled the determination of the exact correlation between macular pathology and the corresponding functional abnormality.

Microperimetry is a psychophysical method that is rapid, safe, non-invasive, and useful for assessing the stability of fixation. Retinal sensitivity can be displayed at only a few normal or abnormal points, with a low retinal sensitivity level. In addition, a stable or unstable fixation visual point should be determined and documented postoperatively to assess the behavior of this fixation pattern over time.

Microperimetry using the MP-3 MAIA Confocal Microperimeter (MetroVision, France), a device routinely used in our retinal unit, should show whether there is a stable or unstable fixation pattern and whether the location is foveocentral or eccentric, and the type of fixation pattern should also be determined and documented. The retinal sensitivity analysis map should be evaluated and correlated after interpretation to determine whether there is abnormal or normal macular integrity with normal or reduced sensitivity, mainly in the center of the fovea. The correlation between the reduced retinal sensitivity locus and corresponding retinal thickness on SD-OCT should also be investigated. The standard protocol that we used covered a 10° diameter area with 37 measurement

points and a light stimulus projected directly over the macula surface, with a Goldman III size stimulus, background luminance of four apostilbs (asb), a maximum luminance of 1000 asb, and a dynamic range of 36 decibels (dB). Fixation stability and location pattern parameters should be assessed by tracking eye movements 25 times per second and plotting the resulting distribution over the scanning laser ophthalmoscope (SLO) image. Each movement is represented by a point and the overall site describes the preferred retinal locus.

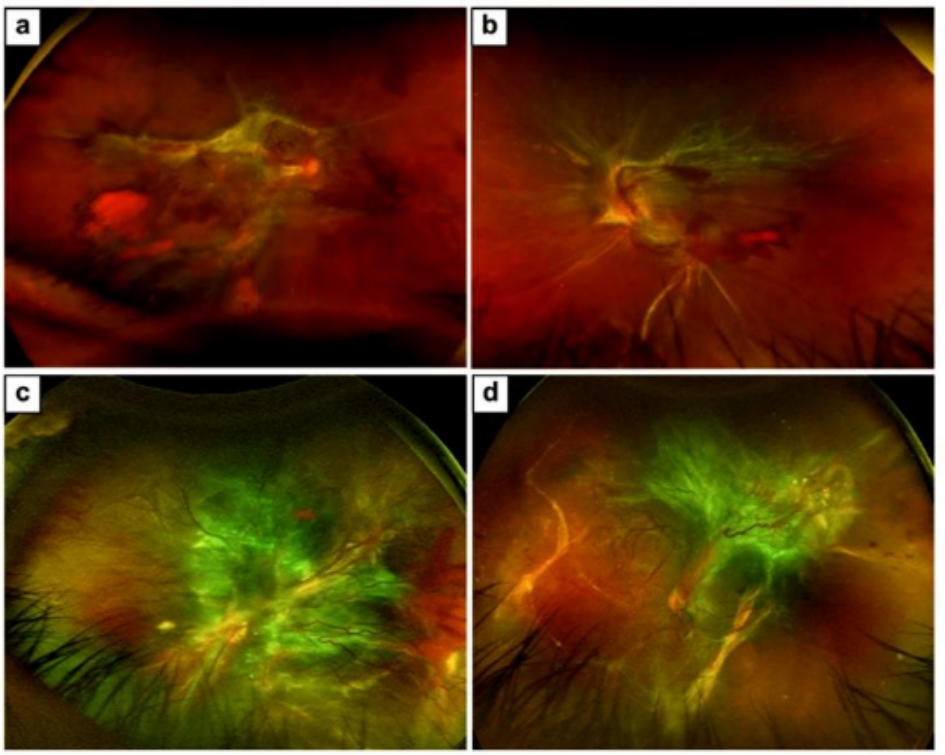

Fig. (2). ***Different types of diabetic TRD.*** (**a**) A wide-field Optos color fundus image of diabetic TRD with macular involvement. The media are clear, proliferative fibrovascular tissue emerges from the optic disc and shows traction elevation of the temporal vascular arcades, and the retina of the posterior pole is detached with the macula involved. The rest of the retina appears thin and atrophic without evidence of prior panretinophotocoagulation (PRP). (**b**) Diabetic TRD where the optic nerve is observed, very extensive TRD is affecting the posterior pole and the macula is detached and heterotopic. Neovascular activity with evidence of localized vitreous hemorrhage is observed without evidence of a previous PRP. (**c**) Magnified wide-field Optos color image of an exuberant fibrovascular tissue proliferation over the posterior pole and along the vascular arcades that contract and detach the macula. (**d**) Another image of diabetic TRD with macular involvement. The TRD extends to the nasal equator of the retina with vertical subretinal demarcation lines. This modified multipanel figure was obtained from a previous publication [27] and is used under the Creative Commons Attribution 4.0 International License (https://creativecommons.org/licenses/by/4.0/).

Computerized mfERG should be used to detect focal (regional) outer retinal abnormalities, and the amplitude and implicit time of the N1 wave, implicit time of the P1 wave, and elevation electroretinography 3-D maps should be assessed in the affected eye and compared to the contralateral eye or to the corresponding normal control normative dataset. The 61-hexagon 30° standardized technique is regularly performed to test the macular electrical multifocal outer layer sensitivity point-to-point at the <2-degree to >15-degree central rings (<2, 2–5, 5–10, 10–15, and >15 central rings) once the postoperative BCVA has been reached. The authors also recommend performing at least 10-2 and 30-2 chromatic campimetry evaluations postoperatively to assess long-term central field function.

Surgical Techniques in Diabetic Tractional Retinal Detachment

The authors preferred to perform the technique using a standard 25-gauge, self-sealed, three-port, control-perfused PPV in all eyes of patients under local anesthesia. Patients should also undergo sedation. In addition to central vitrectomy, triamcinolone acetonide (Kenalog 40 mg/mL; Bristol-Myers, New York, NY, USA)-assisted removal of the cortical vitreous from the surface of the retina should be performed using a silicone-tipped cannula and active suction, paying special attention to the detection of macular preretinal fibrovascular proliferation. Removal of the hyaloid in cases of complex vitreoretinal interface requires a combination of delamination alternating with segmentation along with visco-dissection techniques for adherent vitreous and epiretinal fibrovascular proliferative tissue, avoiding iatrogenic retinal breaks. Any foci of perfused retinal neovascularization or bleeding from the retinal vasculature should be treated to maintain hemostasis throughout the procedure. Once the hyaloid is carefully dissected and removed, attention should be shifted to fibrovascular membrane dissection using visco-dissection, segmentation, and/or delamination techniques, and residual epiretinal tissue should be peeled or dissected to release macular traction and distortion. After removal of the anterior-posterior traction, the focus should be maintained on tangential or circumferential traction, and surgical macular evaluation and revision should be performed in all cases using 0.15% trypan blue ophthalmic solution (Membrane Blue; Dutch Ophthalmic, USA) as an adjuvant dye to stain cortical vitreous remnants or epiretinal macular membranes. In cases showing membrane epiretinal proliferation, a mixture of 0.15 mL of a 0.25 mg/mL (0.025%) diluted isomolar solution (pH 7.4) of Brilliant Blue G (BBG) dye is recommended to selectively stain the ILM because of the suspected traction contribution of ERM proliferation. Once the tractional components are released, rhegmatogenous lesions, if any, should be diathermally marked, macular reattachment should be achieved, and argon laser-assisted scatter panretinal photocoagulation (PRP) should be performed. In cases without rhegmatogenous lesions, PRP should be applied to avoid areas of subretinal fluid that may induce

small retinal breaks (Fig. **4a** to **f**); (Fig. **5a - c** and **h - i**). A selected tamponade, such as a long-acting nonexpandable perfluoropropane (C_3F_8) gas mixture at 15%, or heavier than water 1000 or 5000 cks (centistokes) silicon oil should be administered at the end of the surgical procedure based on the experience and preference of the surgeon.

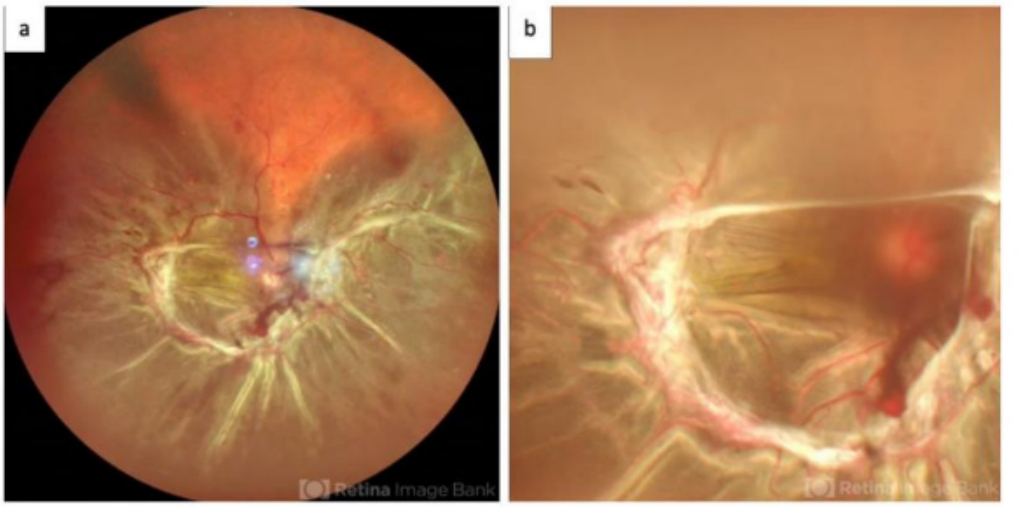

Fig. (3). ***Different types of diabetic TRD.*** (**a**) Severe macula-off diabetic tractional retinal detachment. 57082. (**b**) Tractional and rhegmatogenous retinal detachment in PDR. 57083. The images in this modified figure were originally published on the Retina Image Bank® website. Manish Nagpal, MD. Photographer Gayathri Mohan. Retina Foundation. Retina Image Bank. Jun 10, 2020. © The American Society of Retina Specialists.

Postoperative Structural and Multimodal Functional Findings in TRD

Graphs **1–6** summarize the functional outcomes previously published by the authors [27].

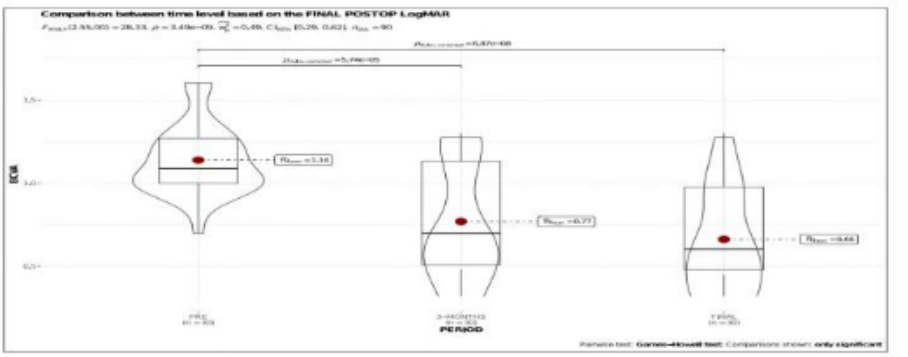

Graph. 1. Comparison between preoperative, 3-month, and final postoperative BCVA.

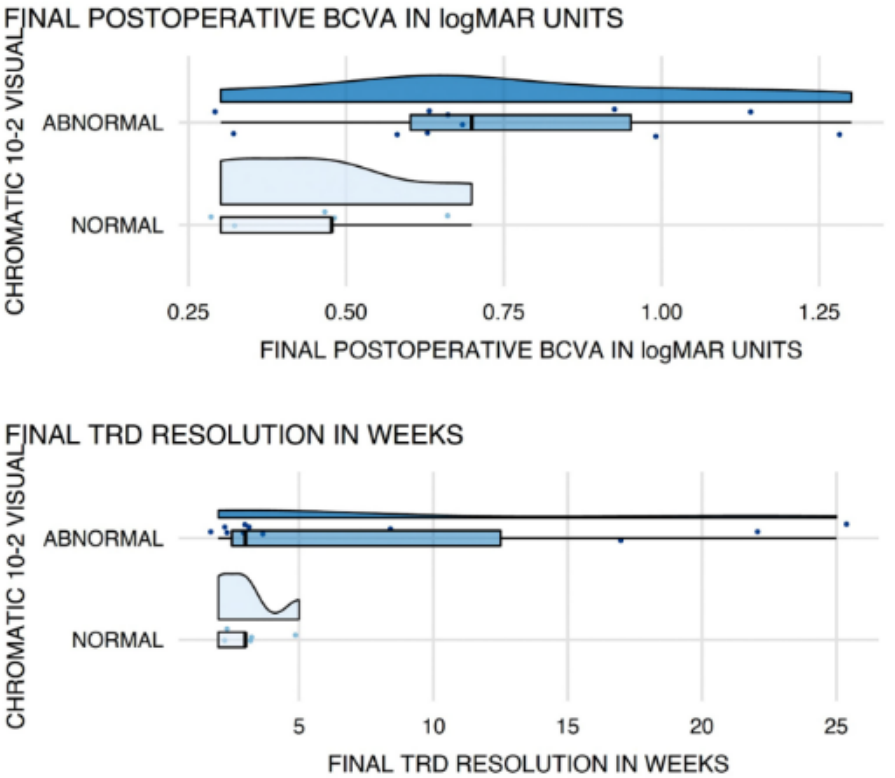

Graph. 6. Comparison of chromatic visual field testing between BCVA and TRD.

For the surgical outcomes of this type of vitreoretinal pathology in patients with diabetes, the authors applied their experiences from the cited publication and further clarified these outcomes by using examples of surgical cases to academically and didactically describe the outcomes of these patients. We used the terminology proposed in the International Nomenclature for Optical Coherence Tomography Panel report to describe the structural preoperative and postoperative SD-OCT findings [28]. The postoperative structural SD-OCT findings (Fig. **5d**, **e**, **j**, and **k**) showed foveal contour profile abnormalities, diffuse retinal layer thinning with CSFT abnormalities, IS/OS disruptions (EZ), and external limiting membrane (ELM) line abnormalities. In the OCT-A evaluation of the subset of 16 post-operated patients, the superficial and deeper capillary vascular plexuses showed extensive perfusion abnormalities, and the choriocapillaris plexus evaluation revealed abnormal choriocapillaris perfusion; the pericapillary foveal net was enlarged, asymmetrical, and irregular, and the quality of vascular density was abnormal (Fig. **4g**, **h** and **5f**, **l**) (Table **1**).

Table 1. Summary of preoperative and postoperative TRD structural and perfusional findings.

SD-OCT (n=30) and OCT-A (n=16) findings:	-	-
Mean time of the preoperative evolution of TRD	11.6 weeks	±2.3 SD
Mean time of the postoperative TRD resolution **Mean time of the postoperative follow-up**	6.2 weeks 11.4 weeks	±2.1 weeks ±5.7 weeks
Postoperative normal contour profile **CSFT abnormalities**	9	30%
Presence of DRIL	13	43.3%
EZ abnormalities	23	76.6%
ELM line abnormalities **Superficial and deep vascular plexus abnormalities**	21	70%
Superficial and deep vascular plexus abnormalities	14	87.5%
Perifoveal capillary net abnormalities	12	75%
Vessel density abnormalities	10	62.5%

TRD, tractional retinal detachment; CSFT, central subfoveal thickness; DRIL, disorganization of the retinal inner layers; EZ, ellipsoid zone; ELM, external limiting membrane. SD-OCT, spectral-domain optical coherence tomography; OCT-A, optical coherence tomography angiography.

Long-term microperimetry assessment in a subset of postoperative eyes showed abnormal macular integrity with reduced retinal sensibility, mainly in the center of the fovea, and reduced retinal sensibility throughout the ischemic areas. This assessment also showed a correlation between SD-OCT macular pathology and the corresponding functional abnormalities, as determined using microperimetry, and the perfused abnormalities observed on OCT-A images (Fig. **4g** and **h**), (Fig. **5f** and **l**), and (Fig. **6d** and **e**). However, no correlation was observed between the localized locus with reduced macular sensitivity and the corresponding retinal thickness on the OCT images. The corresponding SD-OCT B-scan and OCT-A images depict epiretinal membrane proliferation and intraretinal vascular patterns, respectively (Fig. **6c**, **d**, and **e**). Chromatic campimetry revealed reduced retinal sensitivity without any specific color-discrimination abnormalities (Fig. **4i**). A deeply abnormal mfERG elevation map was observed in a small set of eyes tested (Fig. **4j**). Reduced mean retinal sensitivity, deeply reduced foveal sensitivity with abnormal fixation stability, and an eccentric location pattern with abnormally decreased retinal sensitivity were the main findings obtained from microperimetry (Fig. **4k**). The mfERG showed outer retinal and photoreceptor abnormalities and ischemic patterns in the middle layers of the retina, as well as a decreased amplitude of the N1 wave and an abnormally prolonged P1 implicit time (Fig. **4 l**) (Table **2**).

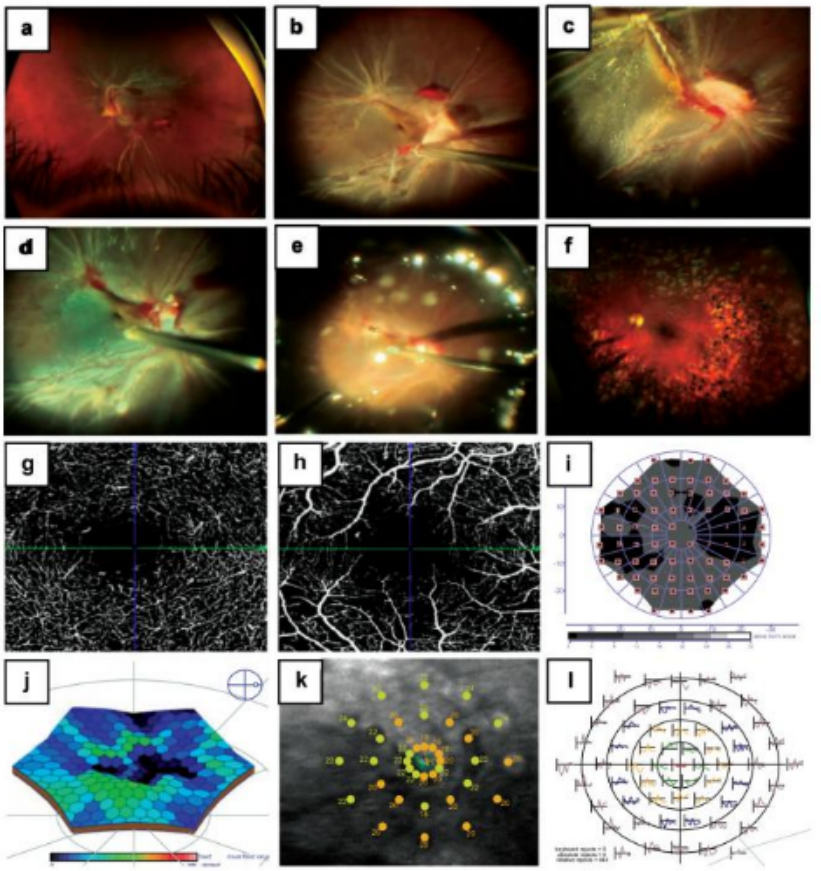

Fig. (4). ***Surgical steps, perfusional and functional findings.*** (**a**) Wide-field Optos color fundus image of an eye with long-evolution type 2 diabetes mellitus and abundant proliferative fibrovascular preretinal tissue that detaches the retina involving the macula. (**b**) Surgical image showing a severe traction detachment, the macula is off and fibrovascular tissue emerges from the optic nerve that detaches detaching the retina and temporal vascular arcades. (**c**) Magnified image showing clear detachment of the macula with the macula dragged and distorted. (**d**) Image depicting the release of the detached macula where trypan blue dye is used to stain vitreous or fibrovascular remnants and facilitate membrane stripping. This surgical image also depicts a distorted and stained macular surface with evidence of dragged macular tissue due proliferative tissue remnants over the optic nerve and along the inferior temporal arcade. (**e**) Surgical image under air where the macula has been released and appears to be reattached, and transoperative argon laser endophotocoagulation marks over the surface of the reattached retina are shown. (**f**) Corresponding final long-term fundus photo of the previous case showing a nicely attached retina. (**g**) En face SD-OCT-A image of the deep vascular plexus (DVP) slab showing an enlarged FAZ area, with some capillary dropouts. (**h**) En face OCT-A image of the SVP slab with countless abnormal capillary terminal segment defects and small zones of capillary dropouts. (**i**) Image depicting an abnormal retinal sensibility on the chromatic central visual field. (**j**) The mfERG is substantially abnormal in the central rings, and the topographic elevation 3-D map is abnormally depressed. (**k**) Image showing an abnormal macular sensitivity on microperimetry. (**l**) The mfERG is substantially abnormal in the central rings, and the topographic elevation 3-D map is abnormally depressed. This modified multipanel figure was obtained from a previous publication [27] and is used under the Creative Commons Attribution 4.0 International License (https://creativecommons.org/licenses/by/4.0/).

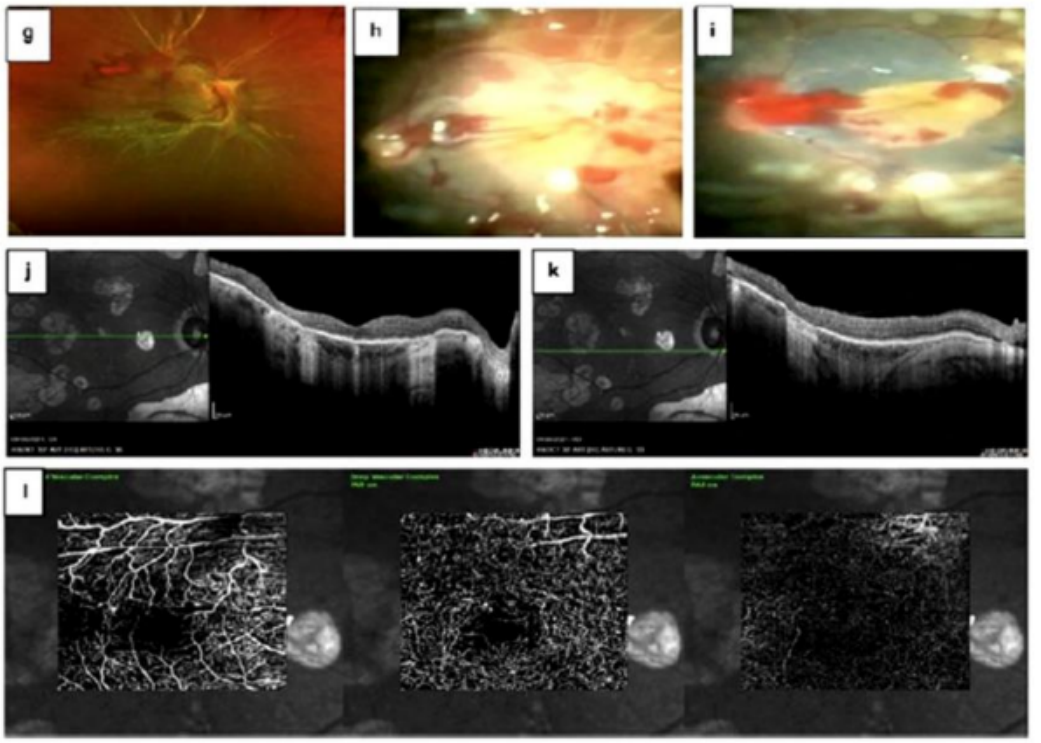

Fig. (5). ***Surgical approach, structural and perfusional outcomes.*** (**a**) Surgical view of a very complex diabetic TRD involving the macula in a hammock configuration. (**b**) The macula was released, and passive blood aspiration and retina exploration were mandatory. (**c**) Image depicting the corresponding appearance of the tissue in the previous image with the retina completely reattached with extensive PRP. (**d**) Image showing diffuse retinal thinning and corresponding laser scarring of the full-thickness retina layers; the macular contour is indistinguishable. (**e**) Corresponding final Spectralis cross-sectional horizontal B-scan depicting a thinner macular profile with diffuse thinning of the macular layers. (**f**) Postoperative en face SD-OCT-A images depicting irregular filling at the level of the SVP, and the DVP insufficiently filled due to a low vessel density (VD) and capillary dropouts with irregular and enlarged perifoveal capillary net. The choriocapillaris is abnormal with compensatory and atypical engorged choroidal vessels. (**g**) Image showing a preoperative extensive diabetic macula-off TRD. (**h**) Image depicting a transoperative view. The retina has been reattached, and some macular traction lines through the macula due to persistent superficial traction are observed. (**i**) Image showing the corresponding stained and removed internal limiting membrane to release the superficial traction mentioned above. (**j**) Image depicting a 4-month postoperative Spectralis cross-sectional horizontal B-scan with PRP laser scars and irregular and diffuse retinal thinning along with a well-recovered macular profile contour, hard-to-identify structural biomarkers and the absence of well-defined retinal inner layer biomarkers. (**k**) Corresponding image obtained at the final follow-up with a better recovered Spectralis cross-sectional horizontal B-scan structural evaluation. The hyper-reflexive effect of the laser scarring is noted. (**l**) En face OCT-A image showing some degree of irregular filling at the level of the SVP and DVP plexuses; note that the choriocapillaris is insufficient. This modified multipanel figure was obtained from a previous publication [27] and is used under the Creative Commons Attribution 4.0 International License (https://creativecommons.org/licenses/by/4.0/).

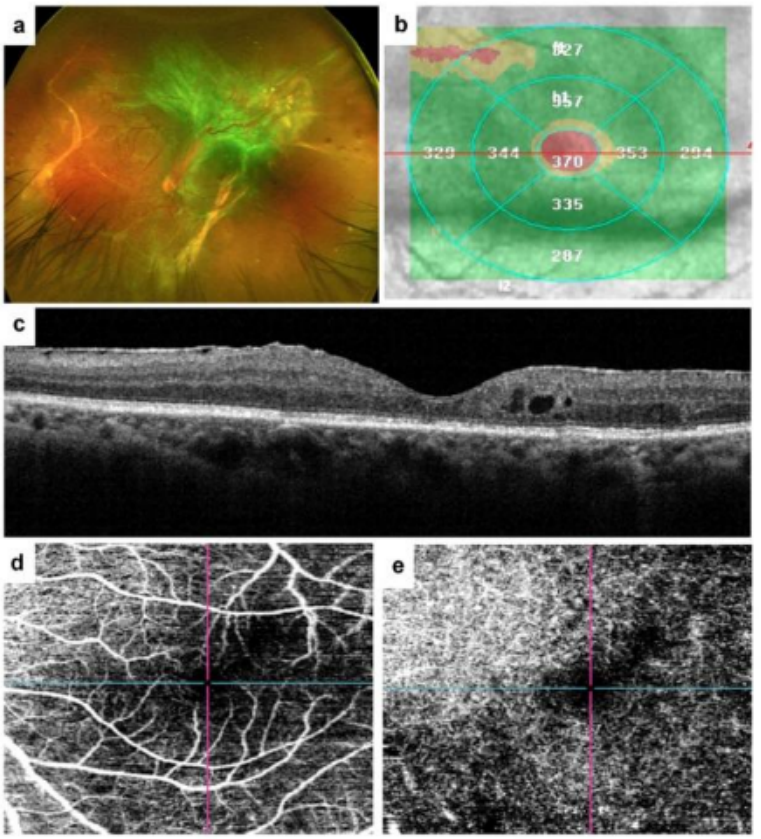

Fig. (6). ***Postoperative structural and perfusional findings***. (**a**) Image depicting a preoperative wide-field Optos color fundus image of a very complex, chronic diabetic macula-off TRD. (**b**) Image with postoperative topographic irregular central macular thickening due to chronic macular edema. (**c**) Postoperative structural cross-sectional horizontal SD-OCT B-Scan image showing a preserved macular profile with some mild superficial wrinkling of the nasal region along with extrafoveal cystic chronic residual edema mainly over the temporal side of the macula. Some external limiting membrane (ELM) line discontinuities are observed, and the EZ is preserved. (**d**) Corresponding postoperative en face SD-OCT-A image of the SVP slab between normal range VD perfusion indices. (**e**) En face SD-OCT-A image of the DVP slab shows some irregularities of the deep macula circulation with an irregular deep juxtafoveal capillary net and an enlarged FAZ area. This modified multipanel figure was obtained from the *International Journal of Ophthalmology & Visual Science*. Vol. 6, No. 4, 2021, pp. 187-198. doi: 10.11648/j.ijovs.20210604.12 and is used under the Creative Commons Attribution 4.0 International License (https://creativecommons.org/licenses/by/4.0/).

Representative Surgical Cases

Surgical Case 1

A 42-year-old male patient with 18 years of type 2 diabetes had irregular metabolic control. His last glycosylated hemoglobin level was 7.7. The patient had proliferative diabetic retinopathy and PRP in both the eyes. The patient

presented with progressive low vision in his right eye at 12 weeks. Ophthalmological examination revealed a pseudophakic RE with cloudy media. The TOA was 16 mmHg with no manifestations of anterior segment neovascularization, signs of moderate vitreous bleeding, and evidence of a fibrovascular tissue stalk that detached the posterior pole, mainly at the level of the macula. B-mode ultrasonography confirmed the diagnosis of diabetic TRD with macular involvement. The patient underwent vitrectomy and endophotocoagulation to achieve uneventful reapplication of the macula. Postoperative evaluation at 14 months showed an abnormal FAZ area on the DVP and SVP slabs (Fig. **7a** and **b**), and postoperative cystic macular edema was detected on B-scan crossline SD-OCT examination (Fig. **7c** and **d**). The en face red-free slab showed superficial extrafoveal macular traction without macular distortion (Fig. **7e**). Quantitative VD evaluation was considered to be within normal limits, as shown in white numbers on the different subfoveal regions on the ETDRS-like grid (Fig. **7f**). Long-term full-thickness macular edema was observed in retinal topography images (Fig. **7g**). The final BCVA was 20/80.

Surgical Case 2

A 59-year-old female patient with chronic complications of proliferative diabetic retinopathy showed evidence of vitreous hemorrhage on several occasions. She was unable to undergo laser photocoagulation satisfactorily, and because of the presence of fibroglial tissue, the patient was not managed preoperatively with bevacizumab therapy. She had experienced significantly low vision for 12 weeks, and ultrasound examination showed complex tractional detachment of the macula (Fig. **8a**). Fifteen months after vitrectomy, she was evaluated using OCT-A. An Angio montage of the papilla and macula showed restored perfusion quite close to normal, with an irregular and enlarged FAZ and interruptions of the capillary margin at the level of the SVP (Fig. **8b** and **c**). The postoperative OCT-A evaluation showed a quantitatively altered VD pattern that was considered lower than normal (Fig. **8d**), the macular topography showed discrete and irregular macular thickening due to refractory edema (Fig. **8e**), which showed important capillary dropouts in the vicinity of the FAZ area that was enlarged, the juxtafoveal capillary net was abnormal in VD, and the long-term VD profiles were quantified as lower than normal (Fig. **8f**). Long-term postoperative horizontal B-scan SD-OCT images showed irregular foveal contours and diffuse irregular macular thickening due to the presence of macular edema, evidence of DRIL, and normal outer retinal biomarkers on OCT images (Fig. **8g**). The final BCVA value was 20/100.

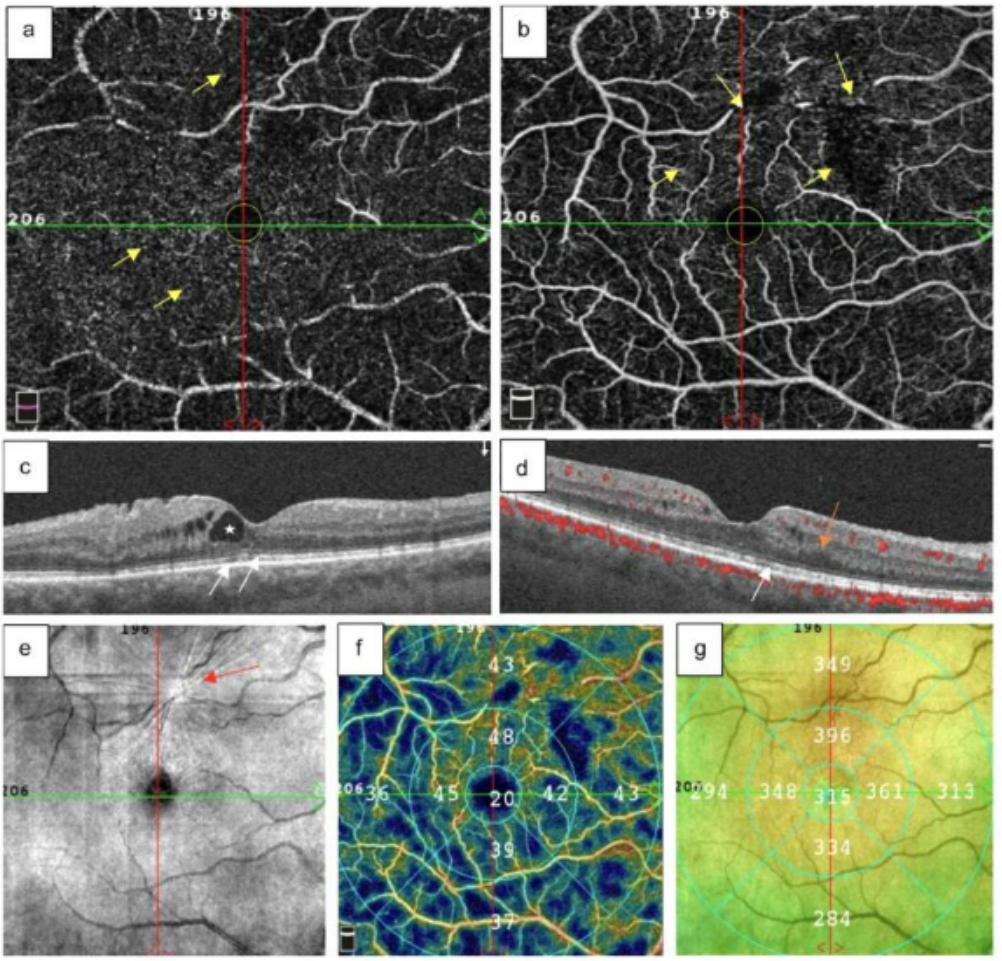

Fig. (7). ***Surgical case 1.*** (**a**) Images depicting irregular deep vascular and SVP slabs with a smaller, preserved and remodeling of the FAZ area. Multiple microcapillary end-vascular dilatations are depicted (yellow arrows). (**b**) The image depicts a vertical B-scan with retinal thickening due to intraretinal edema (white asterisk), DRIL (white arrows) and discontinuities over the EZ (yellow arrows) and external limiting membrane. (**c**) Postoperative vertical B-scan depicting an abnormal foveal contour profile, diffuse thickening of the macula due to intraretinal edema (white asterisk), some DRIL and some discontinuities (white arrows) of the EZ. (**d**) Postoperative horizontal B-scan depicting an abnormal foveal contour profile, diffuse thickening of the macula, DRIL (orange arrow) and some discontinuities (white arrows) of the EZ. The red dots represent retinal and choroidal vessels. (**e**) A red free SLO segmentation en face image and a superficial traction epicenter (red arrow) are observed. (**f**) Image depicting a lower vessel density in the 9-grid-based measurements, with the value shown in white numbers over each subfield. (**g**) Corresponding postoperative full-thickness macular topography image showing diffuse retinal thickening. This modified multipanel figure was obtained from the *International Journal of Ophthalmology & Visual Science*. Vol. 6, No. 4, 2021, pp. 187-198. doi: 10.11648/j.ijovs.20210604.12 and is used under the Creative Commons Attribution 4.0 International License (https://creativecommons.org/licenses/by/4.0/).

Surgical Case 3

A 57-year-old male patient with diabetes for 22 years presented with progressively decreasing vision in the left eye at 14 weeks of evolution, with no history of laser photocoagulation or antiangiogenic therapy. Ophthalmoscopic examination and B-mode ultrasound showed severe and extensive tractional detachment of the macula (Fig. **9a**). The patient underwent uneventful PPV and phacoemulsification with surgical reattachment of the macula without complications. At 19 months postoperatively, a perfusion evaluation was performed using SD-OCT-A, showing an SVP with multiple high-grade vascular deficiencies in the VD evaluation, an abnormally enlarged FAZ area, and loss of shape of the corresponding juxtafoveal capillary net (Fig. **9b**). The long-term postoperative crossline SD-OCT examination showed severe diffuse total irregular thickening of the macula, several large confluent intraretinal macrocysts, alterations in the microstructure, and the presence of severe extrafoveal and subfoveal DRIL; biomarkers of the outer retinal layer were not recognizable. The vertical B-scan image of the macula shows full-thickness ischemic edema with a loss of biomarkers (Fig. **9c** and **d**). The surface topography of the superficial retina was abnormal and irregular in thickness (Fig. **9e**), and the quantitative evaluation of the VD pattern was considered to be lower than normal (Fig. **9f**). The final BCVA of the eyes was 20/160.

Surgical Case 4

A 46-year-old female patient with a rapid and progressive loss of vision of 6 weeks of evolution, diabetes mellitus for 21 years with good glycemic control and a glycosylated hemoglobin level of 8.7 was diagnosed with macula-off TRD. Because the macula was involved (Fig. **10a**), the preoperative SD-OCT allowed us to appreciate the complexity of the vitreoretinal interface in the presence of abundant epi-and preretinal membranes and abundant subretinal fluid (Fig. **10b**). The patient underwent PPV surgery and laser endophotocoagulation. Eight weeks postoperatively, significant vitreous bleeding was identified with redetachment of the macula, for which she underwent vitrectomy revision with successful and uneventful reapplication of the macula. The final quantitative postoperative evaluation at 23 months showed several areas of lower-than-normal VD values (Fig. **10c**), irregular thickening of the superficial layers of the retina in the surface topography of the macula (Fig. **10d**), the full-thickness topography of the macula evidenced moderate and uniform thickening of the macula (Fig. **10e**), the VD was deficient quantitatively with several areas of lower-than-normal VD values, the SVP showed substantial alterations in the microcirculation, capillary closures and an enlarged avascular FAZ without precise limits to be measured (Fig. **10f**), The DVP was significantly altered and important capillary closures were observed

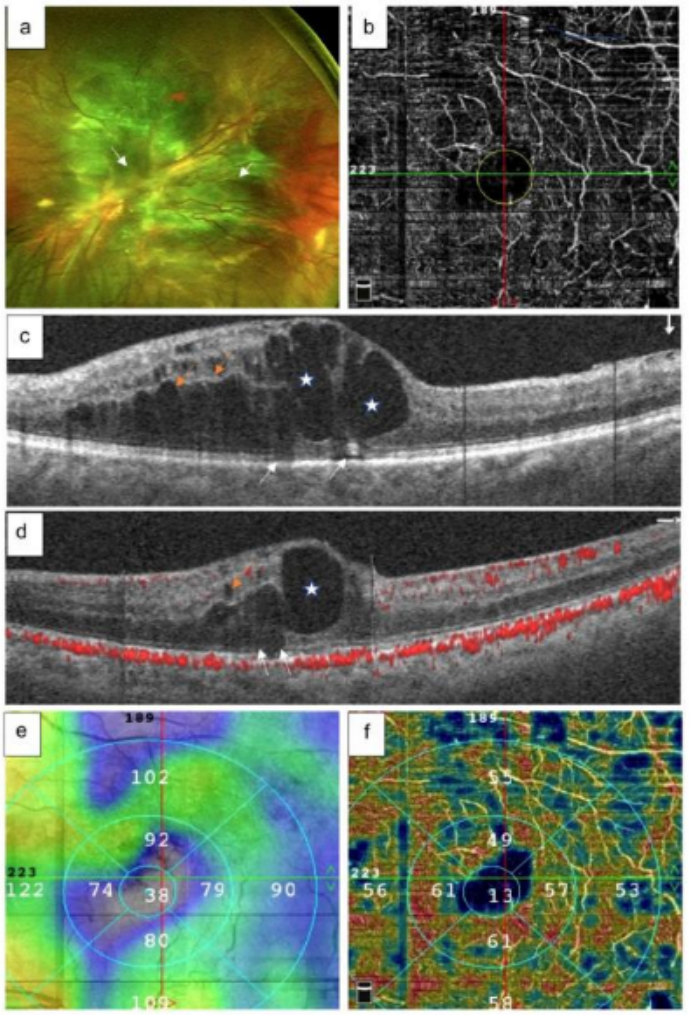

Fig. (9). Surgical case 3. (**a**) Wide-field color photo depicts an extensive diabetic TRD (white arrows). (**b**) Image depicts an abnormal irregular SVP slab with many abnormal capillary segments, microvascular dilation and an enlarged FAZ (yellow circle); some mild saccadic eye movement artifacts are observed. (**c**) Cross-sectional vertical B-scan SD-OCT image shows severe macular thickening and large cystic formation (white asterisks), severe postoperative and persistent DRIL (orange arrows) and the severe disruption of the outer retina OCT biomarkers (EZ and ELM line) (white arrows). The red dots depict the tomographic retinal vessels and the choroidal capillaries. (**d**) Cross-sectional horizontal B-scan SD-OCT image with macular thickening and cystic formation (white asterisk), severe postoperative and persistent DRIL (orange arrows) and severe disruption of the outer retinal SD-OCT biomarkers (EZ and ELM line) (white arrows). The red dots depict the tomographic retinal vessels and the choroidal capillaries. (**e**) The image shows the superficial irregular macular partial-thickness macula topography. (**f**) Image corresponds to the abnormal VD segmentation data acquired over the different macular subfields, with the quantified VD presented in white numbers. This modified multipanel figure was obtained from the *International Journal of Ophthalmology & Visual Science*. Vol. 6, No. 4, 2021, pp. 187-198. doi: 10.11648/j.ijovs.20210604.12 and is used under the Creative Commons Attribution 4.0 International License (https://creativecommons.org/licenses/by/4.0/).

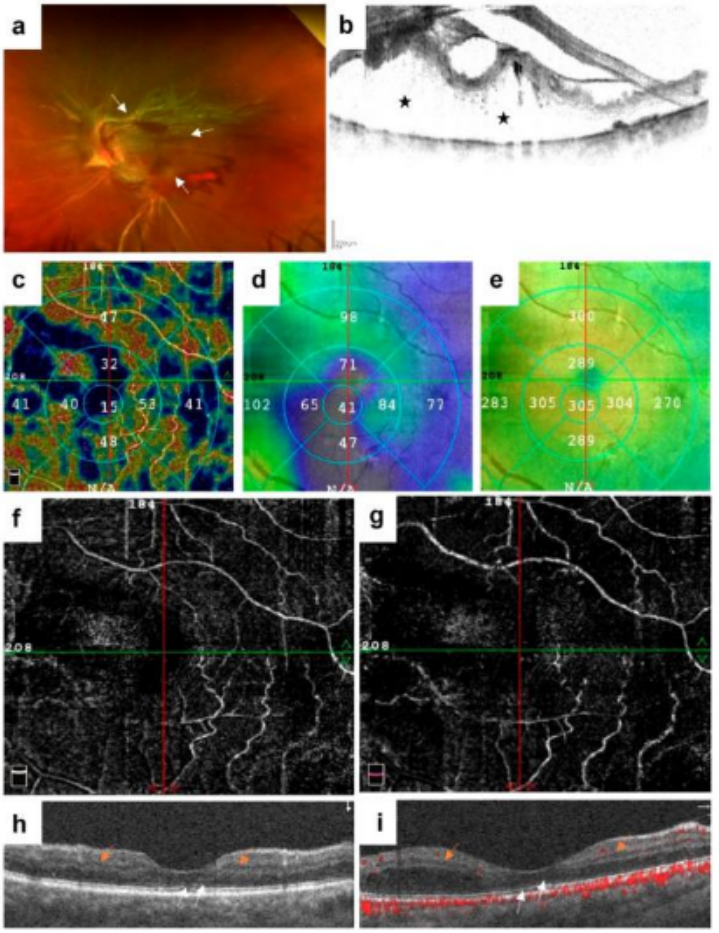

Fig. (10). Surgical case 4. (**a**) Wide-field color photo of the left eye with a severe macula-off diabetic TRD (white arrows). (**b**) The image depicts a preoperative cross-sectional horizontal B-scan SD-OCT with a complex vitreoretinal interface and abundant subretinal fluid (black asterisks). SD-OCT biomarkers were not identified. (**c**) Image depicts an abnormal quantitative VD image at the different macular subfields with the quantification shown in white numbers in each subfield of the macula. (**d**) Image depicts the postoperative partial-thickness abnormal superficial macular topography. (**e**) Image shows the corresponding postoperative full-thickness uniformly thick macular topography. (**f**) The image shows very abnormal microcirculation at the level of the SVP. The quantitation of characteristics of the FAZ area were impossible to detect, and VD perfusion indices were lower than the mean. (**g**) Image depicts the DVP with countless microvascular perfusional abnormalities. The juxtafoveal capillary net and the foveal avascular zone were not identified, and the perfusion indices were lower than the mean on the quantitative evaluation. (**h**) and (**i**) Images depicts a crossline SD OCT B-scan through the center of the fovea. An abnormal foveal contour and diffuse macular thickening were observed, along with the presence of DRIL (orange arrows). The EZ and ELM showed irregularities and discontinuities at the subfoveal level (white arrow). The red dots indicate retinal vessels and choroidal capillaries. Extrafoveal residual subretinal fluid was observed. This modified multipanel figure was obtained from the *International Journal of Ophthalmology & Visual Science*. Vol. 6, No. 4, 2021, pp. 187-198. doi: 10.11648/j.ijovs.20210604.12 and is used under the Creative Commons Attribution 4.0 International License (https://creativecommons.org/licenses/by/4.0/).

consequence of ischemia at the level of the deep capillary plexus. Researchers have not determined whether reversibility potentially declines with increasing duration of DRIL or whether it can be induced, but these findings would have important implications in the timing of macula-off diabetic TRD surgery.

Histologically, the process by which DRIL is represented remains unknown. We presume that it may be a distinct biomarker of tissue damage or poor tissue recovery. To the best of our knowledge, the mechanisms by which DRIL affects BCVA have not yet been determined; therefore, further histological assessments are required. However, the findings analyzed in this case series report [27] and in the literature reviewed [20, 21, 26, 32 - 37] suggested that an increased DRIL length and possibly less viable remaining tissue are associated with worse visual outcomes.

Previous reports on PDR have shown that disruption of the outer retina, mainly the EZ and ELM line biomarkers, are significant predictors of visual prognosis [34, 35, 38]. We consider that the length of the subfoveal DRIL, the integrity of the ELM line, and EZ characteristics correlate well with the longitudinal functional evolution and would predict final visual outcomes [27]. The limited number of patients who were subjected to chromatic central visual field testing showed different degrees of central visual field abnormalities in macular sensibility on the 10-2 and 30.2 VF tests without showing any special cone-selected color discrimination abnormalities. Moreover, in a previously published paper [27], a final BCVA less than 20/200 (1.00 in logMAR units) was ultimately achieved, which was consistent with the findings in the revised literature, and the 10-2 and 30-2 visual field test results were also substantially abnormal. However, certain perfusion indices, such as VD, at different subregions of the macula according to the ETDRS grid and some structural biomarkers, such as DRIL, are important for monitoring once the macula has been successfully reattached. Another important issue is that when the macula becomes detached, it must be managed in a timely manner to ensure that perfusion, mainly of the outer layers, is resumed. Long-term postoperative multimodal evaluation is mandatory to better evaluate the results obtained when timely surgical management is instituted in patients with macula-off diabetic TRD.

The choroid is a highly vascularized tissue that provides an essential blood supply to the RPE and outer retina [39]. Restricted blood supply to the choroid may adversely affect the outer retina, potentially disrupting tissue homeostasis and causing chorioretinal tissue damage.

The choroidal vascularity index (CVI) is a recently introduced quantification parameter that represents the vascular status of the choroid based on OCT images

[40]. CVI was developed as a more precise and robust measurement of choroidal vascularity than previous measurements (such as choroidal vessel diameter and choroidal thickness), which has important limitations [41]. Variations in CVI can be used as an indicator of choroidal vasculature changes, but it cannot capture choriocapillaris flow, which is an important characteristic of choroidal vasculature [42].

CVI has proven to be informative in revealing the status of the choroidal vasculature in a variety of diseases and treatment conditions [43 - 48].

In the diabetic patient, the choroid is an important vascular structure that functions in providing nutrients to the outer retina layers, including the photoreceptors layer [49, 50]. *In vivo*, noninvasive observation of the choroid is relevant to both disease diagnosis and treatment but can be challenging because this structure is located beneath multiple layers of tissue. Recent advancements in OCT and the introduction of OCT angiography have substantially improved our ability to visualize the choroid [49].

Recently, better visualization of the choroid has resulted in innovations in the quantitative evaluation of the choroidal vasculature. CVI, first introduced by Agrawal *et al.* in 2016, is a relatively new biomarker for choroidal vasculature [40]. This approach was developed based on the need for a more accurate assessment of choroidal layers [41]. Since the introduction of this metric, the application of CVI has gained popularity. Additionally, CVI has been applied to a diverse array of retinal diseases, such as diabetic choroidopathy, uveitis, central serous chorioretinopathy, retinal vein occlusion, and many other conditions [40, 44, 51 - 53]. Recent reports have shown that CVI is a promising biomarker for the diagnosis and follow-up evaluation of retinal diseases, among which diabetic retinopathy and postoperative perfusional evaluation in severe TRD cases stand out [54].

CONCLUDING REMARKS

In this chapter, we have attempted to correlate DRIL resolution, SD-OCT structural findings, and other OCT-A vascular plexus outcomes with physiological, structural, and functional parameters. Some patients' eyes showed recovery of structural biomarkers with improved VD perfusion indices and capillary structuring at the level of the vascular plexuses in the macula. The foveal area remained irregular and enlarged without recovery data, indicating some prognostic value that might correlate with the worst final visual acuity. However, the data obtained from microperimetry, chromatic visual field, and mfERG analyses did not lead to conclusive findings due to the small subset of eyes included in reliable postoperative studies used in the corresponding statistical

INL	Inner nuclear layer
IS/OS	Inner segment/outer segment
logMAR	Logarithm of the minimum angle of resolution
mfERG	Multifocal electroretinography
MAIA	Macular Integrity Assessment
MRS	Macular retinal sensitivity
OCT-A	Optical coherence tomography angiography
OPL	Outer plexiform layer
PDR	Proliferative diabetic retinopathy
PPV	Pars plana vitrectomy
PFO	Perfluoro-n-octane
PRP	Panretinal photocoagulation
RRD	Rhegmatogenous retinal detachment
RPE	Retinal pigment epithelium
RSAM	Retinal sensitivity analysis mapping
SO	Silicon oil
SLO	Scanning laser ophthalmoscope
SSI	Signal strength index
SVP	Superficial vascular plexus
TRD	Traction retinal detachment
VA	Visual acuity
VD	Vessel density
VEGF	Vascular endothelial growth factor
VH	Vitreous hemorrhage
VT	Vessel tortuosity

ACKNOWLEDGMENTS

We express our deep appreciation to the technical staff of the Retina Specialists Unit at Oftalmologia Integral ABC (Nonprofit Medical and Surgical Organization) affiliated with The Postgraduate Division Studies at the National Autonomous University of Mexico.

DISCLAIMER

All scientific comments issued in this chapter are solely the responsibility of the authors and not of the institutions with which they are affiliated. This chapter is an

extended and modified version of an article published by the same author(s) in the following journal. J Ophthalmol Clin Res 8:131. 2021 doi.org/10.23937/2378-346X/1410131.

REFERENCES

[1] Echouffo-Tcheugui JB, Dagogo-Jack S. Preventing diabetes mellitus in developing countries. Nat Rev Endocrinol 2012; 8(9): 557-62.
[http://dx.doi.org/10.1038/nrendo.2012.46] [PMID: 22488646]

[2] Kempen JH, O'Colmain BJ, Leske MC, Haffner SM, Klein R, Moss SE. The prevalence of diabetic retinopathy among adults in the United States. Arch ophthal 2004; 122(4): 552-63.

[3] Cruz-Iñigo YJ, Acabá LA, Berrocal MH. Surgical management of retinal diseases: Proliferative diabetic retinopathy and traction retinal detachment. Dev Ophthalmol 2014; 54: 196-203.
[http://dx.doi.org/10.1159/000360467] [PMID: 25196770]

[4] Sharma S, Mahmoud TH, Hariprasad SM. Surgical management of proliferative diabetic retinopathy. Ophthalmic Surg Lasers Imaging Retina 2014; 45(3): 188-93.
[http://dx.doi.org/10.3928/23258160-20140505-01] [PMID: 24840530]

[5] Centers for Disease Control and Prevention (CDC). Blindness caused by diabetes--Massachusetts, 1987-1994. MMWR Morb Mortal Wkly Rep 1996; 45(43): 937-41.
[PMID: 8927019]

[6] Salam A, Mathew R, Sivaprasad S. Treatment of proliferative diabetic retinopathy with anti-VEGF agents. Acta Ophthalmol 2011; 89(5): 405-11.
[http://dx.doi.org/10.1111/j.1755-3768.2010.02079.x] [PMID: 21294854]

[7] Barzideh N, Johnson TM. Subfoveal fluid resolves slowly after pars plana vitrectomy for tractional retinal detachment secondary to proliferative diabetic retinopathy. Retina 2007; 27(6): 740-3.
[http://dx.doi.org/10.1097/IAE.0b013e318030c663] [PMID: 17621183]

[8] Sivaprasad S, Prevost AT, Bainbridge J, *et al.* Clinical efficacy and mechanistic evaluation of aflibercept for proliferative diabetic retinopathy (acronym CLARITY): A multicentre phase IIb randomised active-controlled clinical trial. BMJ Open 2015; 5(9): e008405.
[http://dx.doi.org/10.1136/bmjopen-2015-008405] [PMID: 26369798]

[9] Fong DS, Strauber SF, Aiello LP, *et al.* Comparison of the modified early treatment diabetic retinopathy study and mild macular grid laser photocoagulation strategies for diabetic macular edema. Arch Ophthalmol 2007; 125(4): 469-80.
[http://dx.doi.org/10.1001/archopht.125.4.469] [PMID: 17420366]

[10] Sivaprasad S, Prevost AT, Vasconcelos JC, *et al.* Clinical efficacy of intravitreal aflibercept versus panretinal photocoagulation for best corrected visual acuity in patients with proliferative diabetic retinopathy at 52 weeks (CLARITY): A multicentre, single-blinded, randomised, controlled, phase 2b, non-inferiority trial. Lancet 2017; 389(10085): 2193-203.
[http://dx.doi.org/10.1016/S0140-6736(17)31193-5] [PMID: 28494920]

[11] Mikhail M, Ali-Ridha A, Chorfi S, Kapusta MA. Long-term outcomes of sutureless 25-G+ pars-plana vitrectomy for the management of diabetic tractional retinal detachment. Graefes Arch Clin Exp Ophthalmol 2017; 255(2): 255-61.
[http://dx.doi.org/10.1007/s00417-016-3442-7] [PMID: 27480177]

[12] Sun JK, Lin MM, Lammer J, *et al.* Disorganization of the retinal inner layers as a predictor of visual acuity in eyes with center-involved diabetic macular edema. JAMA Ophthalmol 2014; 132(11): 1309-16.
[http://dx.doi.org/10.1001/jamaophthalmol.2014.2350] [PMID: 25058813]

[13] Gorczynska I, Migacz JV, Zawadzki RJ, Capps AG, Werner JS. Comparison of amplitude-decorrelation, speckle-variance and phase-variance OCT angiography methods for imaging the human

retina and choroid. Biomed Opt Express 2016; 7(3): 911-42.
[http://dx.doi.org/10.1364/BOE.7.000911] [PMID: 27231598]

[14] Gill A, Cole ED, Novais EA, *et al.* Visualization of changes in the foveal avascular zone in both observed and treated diabetic macular edema using optical coherence tomography angiography. Int J Retina Vitreous 2017; 3(1): 19.
[http://dx.doi.org/10.1186/s40942-017-0074-y] [PMID: 28642823]

[15] Yannuzzi LA, Rohrer KT, Tindel LJ, *et al.* Fluorescein angiography complication survey. Ophthalmology 1986; 93(5): 611-7.
[http://dx.doi.org/10.1016/S0161-6420(86)33697-2] [PMID: 3523356]

[16] Ho AC, Yannuzzi LA, Guyer DR, Slakter JS, Sorenson JA, Orlock DA. Intraretinal leakage of indocyanine green dye. Ophthalmology 1994; 101(3): 534-41.
[http://dx.doi.org/10.1016/S0161-6420(94)31323-6] [PMID: 7510380]

[17] Hwang TS, Zhang M, Bhavsar K, *et al.* Visualization of 3 distinct retinal plexuses by projection-resolved optical coherence tomography angiography in diabetic retinopathy. JAMA Ophthalmol 2016; 134(12): 1411-9.
[http://dx.doi.org/10.1001/jamaophthalmol.2016.4272] [PMID: 27812696]

[18] Spaide RF, Klancnik JM Jr, Cooney MJ, *et al.* Volume-rendering optical coherence tomography angiography of macular telangiectasia type 2. Ophthalmology 2015; 122(11): 2261-9.
[http://dx.doi.org/10.1016/j.ophtha.2015.07.025] [PMID: 26315043]

[19] Matsunaga D, Yi J, Puliafito CA, Kashani AH. OCT angiography in healthy human subjects. Ophthalmic Surg Lasers Imaging Retina 2014; 45(6): 510-5.
[http://dx.doi.org/10.3928/23258160-20141118-04] [PMID: 25423629]

[20] Tan PEZ, Balaratnasingam C, Xu J, *et al.* Quantitative comparison of retinal capillary images derived by speckle variance optical coherence tomography with histology. Invest Ophthalmol Vis Sci 2015; 56(6): 3989-96.
[http://dx.doi.org/10.1167/iovs.14-15879] [PMID: 26098464]

[21] Huang D, Jia Y, Gao SS, Lumbroso B, Rispoli M. Optical coherence tomography angiography using the optovue device. Dev Ophthalmol 2016; 56: 6-12.
[http://dx.doi.org/10.1159/000442770] [PMID: 27022989]

[22] Kwiterovich KA, Maguire MG, Murphy RP, *et al.* Frequency of adverse systemic reactions after fluorescein angiography. Results of a prospective study. Ophthalmology 1991; 98(7): 1139-42.
[http://dx.doi.org/10.1016/S0161-6420(91)32165-1] [PMID: 1891225]

[23] Bhavsar AR, Torres K, Glassman AR, Jampol LM, Kinyoun JL, Network DRCR. Evaluation of results 1 year following short-term use of ranibizumab for vitreous hemorrhage due to proliferative diabetic retinopathy. JAMA Ophthalmol 2014; 132(7): 889-90.
[http://dx.doi.org/10.1001/jamaophthalmol.2014.287] [PMID: 25010170]

[24] de Carlo TE, Bonini Filho MA, Baumal CR, *et al.* Evaluation of preretinal neovascularization in proliferative diabetic retinopathy using optical coherence tomography angiography. Ophthalmic Surg Lasers Imaging Retina 2016; 47(2): 115-9.
[http://dx.doi.org/10.3928/23258160-20160126-03] [PMID: 26878443]

[25] Matsunaga DR, Yi JJ, De Koo LO, Ameri H, Puliafito CA, Kashani AH. Optical coherence tomography angiography of diabetic retinopathy in human subjects. Ophthalmic Surg Lasers Imaging Retina 2015; 46(8): 796-805.
[http://dx.doi.org/10.3928/23258160-20150909-03] [PMID: 26431294]

[26] Ishibazawa A, Nagaoka T, Takahashi A, Omae T, Tani T, Sogawa K. Optical coherence tomography angiography in diabetic retinopathy: A prospective pilot study. Am Jophthal 2015; 160(1): 35-44.e1.
[http://dx.doi.org/10.1016/j.ajo.2015.04.021]

[27] Quiroz-Reyes M, Quiroz-Gonzalez E, Esparza-Correa F, Kim-Lee J, Morales-Navarro J. Outcomes for

successfully repaired macula-off diabetic tractional retinal detachment. Int J Ophthalmol Clin Res 2021; 8: 131.

[28] Staurenghi G, Sadda S, Chakravarthy U, Spaide RF. Proposed lexicon for anatomic landmarks in normal posterior segment spectral-domain optical coherence tomography: The IN•OCT consensus. Ophthalmology 2014; 121(8): 1572-8.
[http://dx.doi.org/10.1016/j.ophtha.2014.02.023] [PMID: 24755005]

[29] Sun JK, Glassman AR, Beaulieu WT, *et al.* Rationale and application of the protocol S anti–vascular endothelial growth factor algorithm for proliferative diabetic retinopathy. Ophthalmology 2019; 126(1): 87-95.
[http://dx.doi.org/10.1016/j.ophtha.2018.08.001] [PMID: 30096354]

[30] Samara WA, Shahlaee A, Adam MK, *et al.* Quantification of diabetic macular ischemia using optical coherence tomography angiography and its relationship with visual acuity. Ophthalmology 2017; 124(2): 235-44.
[http://dx.doi.org/10.1016/j.ophtha.2016.10.008] [PMID: 27887743]

[31] Hsieh YT, Alam MN, Le D, *et al.* OCT angiography biomarkers for predicting visual outcomes after ranibizumab treatment for diabetic macular edema. Ophthalmol Retina 2019; 3(10): 826-34.
[http://dx.doi.org/10.1016/j.oret.2019.04.027] [PMID: 31227330]

[32] Freiberg FJ, Pfau M, Wons J, Wirth MA, Becker MD, Michels S. Optical coherence tomography angiography of the foveal avascular zone in diabetic retinopathy. Graefes Arch Clin Exp Ophthalmol 2016; 254(6): 1051-8.
[http://dx.doi.org/10.1007/s00417-015-3148-2] [PMID: 26338819]

[33] Hwang TS, Gao SS, Liu L, *et al.* Automated quantification of capillary nonperfusion using optical coherence tomography angiography in diabetic retinopathy. JAMA Ophthalmol 2016; 134(4): 367-73.
[http://dx.doi.org/10.1001/jamaophthalmol.2015.5658] [PMID: 26795548]

[34] Ishibashi T, Sakimoto S, Shiraki N, Nishida K, Sakaguchi H, Nishida K. Association between disorganization of retinal inner layers and visual acuity after proliferative diabetic retinopathy surgery. Sci Rep 2019; 9(1): 12230.
[http://dx.doi.org/10.1038/s41598-019-48679-z] [PMID: 31439887]

[35] Shin HJ, Lee SH, Chung H, Kim HC. Association between photoreceptor integrity and visual outcome in diabetic macular edema. Graefes Arch Clin Exp Ophthalmol 2012; 250(1): 61-70.
[http://dx.doi.org/10.1007/s00417-011-1774-x] [PMID: 21874345]

[36] Moein HR, Novais EA, Rebhun CB, *et al.* Optical coherence tomography angiography to detect macular capillary ischemia in patients with inner retinal changes after resolved diabetic macular edema. Retina 2018; 38(12): 2277-84.
[http://dx.doi.org/10.1097/IAE.0000000000001902] [PMID: 29068912]

[37] Durbin MK, An L, Shemonski ND, *et al.* Quantification of retinal microvascular density in optical coherence tomographic angiography images in diabetic retinopathy. JAMA Ophthalmol 2017; 135(4): 370-6.
[http://dx.doi.org/10.1001/jamaophthalmol.2017.0080] [PMID: 28301651]

[38] Tortorella P, D'Ambrosio E, Iannetti L, De Marco F, La Cava M. Correlation between visual acuity, inner segment/outer segment junction, and cone outer segment tips line integrity in uveitic macular edema. BioMed res int 2015; 2015.

[39] Borrelli E, Sarraf D, Freund KB, Sadda SR. OCT angiography and evaluation of the choroid and choroidal vascular disorders. Prog Retin Eye Res 2018; 67: 30-55.
[http://dx.doi.org/10.1016/j.preteyeres.2018.07.002] [PMID: 30059755]

[40] Agrawal R, Gupta P, Tan KA, Cheung CMG, Wong TY, Cheng CY. Choroidal vascularity index as a measure of vascular status of the choroid: Measurements in healthy eyes from a population-based study. Sci Rep 2016; 6(1): 21090.
[http://dx.doi.org/10.1038/srep21090] [PMID: 26868048]

[41] Betzler BK, Ding J, Wei X, *et al.* Choroidal vascularity index: A step towards software as a medical device. Br J Ophthalmol 2022; 106(2): 149-55.
[http://dx.doi.org/10.1136/bjophthalmol-2021-318782] [PMID: 33514528]

[42] Singh RB, Perepelkina T, Testi I. Imaging-based assessment of choriocapillaris: A comprehensive review. Semin Ophthalmol Taylor & Francis 2022; 0(0): 1-22.
[PMID: 35982638]

[43] Foo VHX, Gupta P, Nguyen QD, *et al.* Decrease in choroidal vascularity index of haller's layer in diabetic eyes precedes retinopathy. BMJ Open Diabetes Res Care 2020; 8(1): e001295.
[http://dx.doi.org/10.1136/bmjdrc-2020-001295] [PMID: 32912848]

[44] Nicolini N, Tombolini B, Barresi C, *et al.* Assessment of diabetic choroidopathy using ultra-widefield optical coherence tomography. Transl Vis Sci Technol 2022; 11(3): 35.
[http://dx.doi.org/10.1167/tvst.11.3.35] [PMID: 35353150]

[45] Dou N, Yu S, Tsui CK, *et al.* Choroidal vascularity index as a biomarker for visual response to antivascular endothelial growth factor treatment in diabetic macular edema. J Diabetes Res 2021; 2021: 1-9.
[http://dx.doi.org/10.1155/2021/3033219] [PMID: 34869776]

[46] Rizzo S, Savastano A, Finocchio L, Savastano MC, Khandelwal N, Agrawal R. Choroidal vascularity index changes after vitreomacular surgery. Acta Ophthalmol 2018; 96(8): e950-5.
[http://dx.doi.org/10.1111/aos.13776] [PMID: 29855162]

[47] Bernabei F, Pellegrini M, Taroni L, *et al.* Choroidal vascular changes after encircling scleral buckling for rhegmatogenous retinal detachment. Eye 2021; 35(9): 2619-23.
[http://dx.doi.org/10.1038/s41433-020-01307-x] [PMID: 33223533]

[48] Chun H, Kim JY, Kwak JH, *et al.* The effect of phacoemulsification performed with vitrectomy on choroidal vascularity index in eyes with vitreomacular diseases. Sci Rep 2021; 11(1): 19898.
[http://dx.doi.org/10.1038/s41598-021-99440-4] [PMID: 34615993]

[49] Invernizzi A, Pellegrini M, Cornish E, Yi Chong Teo K, Cereda M, Chabblani J. Imaging the choroid: From indocyanine green angiography to optical coherence tomography angiography. Asia Pac J Ophthalmol 2020; 9(4): 335-48.
[http://dx.doi.org/10.1097/APO.0000000000000307] [PMID: 32739938]

[50] Dolz-Marco R, Gallego-Pinazo R, Dansingani KK. The history of the choroid.Choroidal disorders academic press. 2017; pp. 1-5.
[http://dx.doi.org/10.1016/B978-0-12-805313-3.00001-6]

[51] Kim M, Ha MJ, Choi SY, Park YH. Choroidal vascularity index in type-2 diabetes analyzed by swept-source optical coherence tomography. Sci Rep 2018; 8(1): 70.
[http://dx.doi.org/10.1038/s41598-017-18511-7] [PMID: 29311618]

[52] Agrawal R, Chhablani J, Tan KA, Shah S, Sarvaiya C, Banker A. Choroidal vascularity index in central serous chorioretinopathy. Retina 2016; 36(9): 1646-51.
[http://dx.doi.org/10.1097/IAE.0000000000001040] [PMID: 27124882]

[53] Aribas YK, Hondur AM, Tezel TH. Choroidal vascularity index and choriocapillary changes in retinal vein occlusions. Graefes Arch Clin Exp Ophthalmol 2020; 258(11): 2389-97. [http://dx.doi.org/10.1007/s00417-020-04886-3] [PMID: 32860575]

[54] Iovino C, Pellegrini M, Bernabei F, *et al.* Choroidal vascularity index: An in-depth analysis of this novel optical coherence tomography parameter. J Clin Med 2020; 9(2): 595. [http://dx.doi.org/10.3390/jcm9020595] [PMID: 32098215]